Available online at www.sciencedirect.com
SCIENCE DIRECT®
Physica C 412–414 (2004) 557–565
PHYSICA C
www.elsevier.com/locate/physc

High critical current density in RE–Ba–Cu–O bulk superconductors with very fine RE_2BaCuO_5 particles

S. Nariki [a,*], N. Sakai [a], M. Murakami [a,b], I. Hirabayashi [a]

[a] *Superconductivity Research Laboratory, ISTEC, 1-10-13 Shinonome, Koto-ku, Tokyo 135-0062, Japan*
[b] *Shibaura Institute of Technology, 3-9-14 Shibaura, Minato-ku, Tokyo 108-8548, Japan*

Received 29 October 2003; accepted 5 January 2004
Available online 1 June 2004

Abstract

We have studied the microstructure and critical current density (J_c) of Gd–Ba–Cu–O and Y–Ba–Cu–O bulk superconductors. The size of RE_2BaCuO_5 (RE211) particles trapped in $REBa_2Cu_3O_y$ (RE123) matrix could be refined by employing ultra-fine RE211 powder as a precursor, which led to high J_c values exceeding 1×10^5 A/cm^2 at 77 K in self-field for Gd–Ba–Cu–O. In the case of Y–Ba–Cu–O, however, the size reduction of Y211 led to inhomogeneous distribution of Y211 particles, in that the volume fraction of Y211 phase largely decreased near a seed crystal. We also studied superconducting properties of (Gd,Y)–Ba–Cu–O bulk material fabricated from precursor of Gd123-Y211. The employment of finely-milled Y211 powders resulted in a dramatic enhancement of J_c values in this system. The maximum J_c value for (Gd,Y)–Ba–Cu–O reached 2.5×10^5 A/cm^2 at 77 K.

PACS: 74.72.Bk; 74.60.Jg; 74.80.B; 85.25.Ly
Keywords: Melt-textured bulk; Critical current density; Microstructure Gd–Ba–Cu–O; Y–Ba–Cu–O

1. Introduction

The critical current density (J_c) of RE–Ba–Cu–O superconductors is strongly dependent on the microstructure. The RE_2BaCuO_5 (RE211) particles dispersed in the superconducting RE-$Ba_2Cu_3O_y$ (RE123) phase act as strong pinning centers, in that J_c increased with decreasing the size of RE211 particles. For the size control of RE211 secondary phase, we have investigated the relationship between the size of RE211 starting powder in RE123/RE211 precursor and the diameter of the resulting RE211 particles in melt-textured samples. Our earlier works on Gd–Ba–Cu–O superconductors revealed that the employment of fine Gd211 starting powder leads to the size reduction of Gd211 inclusions dispersed in Gd123 matrix, enhancing the J_c values for melt-textured bulk [1,2]. Large single-grain Gd–Ba–Cu–O samples with excellent J_c properties can function as strong quasi-permanent magnets [3–6]. The melt-textured Gd–Ba–Cu–O 65 mm in diameter can trap an extremely high magnetic flux

* Corresponding author. Tel.: +81-3-3536-5716/5707; fax: +81-3-3536-5705/5717.
E-mail address: nariki@istec.or.jp (S. Nariki).

0921-4534/$ - see front matter © 2004 Elsevier B.V. All rights reserved.
doi:10.1016/j.physc.2004.01.078

density of 3.05 T at 77 K, when the sample was fabricated in a reduced oxygen atmosphere [7]. Therefore, we believe that the employment of fine RE211 starting powder is effective in synthesizing high performance RE–Ba–Cu–O bulk superconductors.

In this paper, we report the fabrication of RE–Ba–Cu–O bulk materials with very fine RE211 particles and their J_c–B properties. We also report on the properties for the Y–Ba–Cu–O and (Gd,Y)–Ba–Cu–O bulk materials fabricated with the employment of finely-milled Y211 powders as starting materials.

2. Refinement of Gd211 particles in Gd–Ba–Cu–O bulk superconductors

In this section, we discuss how the size of Gd211 starting powders affects the microstructure for Gd–Ba–Cu–O bulk samples. As listed in Table 1, three kinds of Gd211 starting powders with different particle sizes were prepared from Gd_2O_3, BaO_2 and CuO powders. The powders of Gd211-A and B were prepared by the calcination of mixed powders at 1050 °C for 4 h and 900 °C for 8 h, respectively. The respective average particle sizes of these powders were 2.7 and 1.0 μm as determined by BET specific area measurements [1]. The Gd211-C was prepared by ball-milling of Gd211-B using ZrO_2–Y_2O_3 balls in acetone for 2 h. The particle size of Gd211-C was reduced to 0.1 μm with this treatment. These Gd211 powders were added to commercial Gd123 powders in a molar ratio of Gd123:Gd211 = 100:40. 0.5 wt% Pt was also added to the mixtures. The mixed powders were uni-axially pressed into pellets 10 mm in diameter and 12 mm in thickness. An MgO(1 0 0) seed was placed at the center top of the pellet,

Table 1
Gd211 starting powders

Powder	Preparation condition	Average particle size (μm)
Gd211-A	Calcination at 1050 °C for 4 h	2.7
Gd211-B	Calcination at 900 °C for 8 h	1.0
Gd211-C	Ball-milling of Gd211-B	0.1

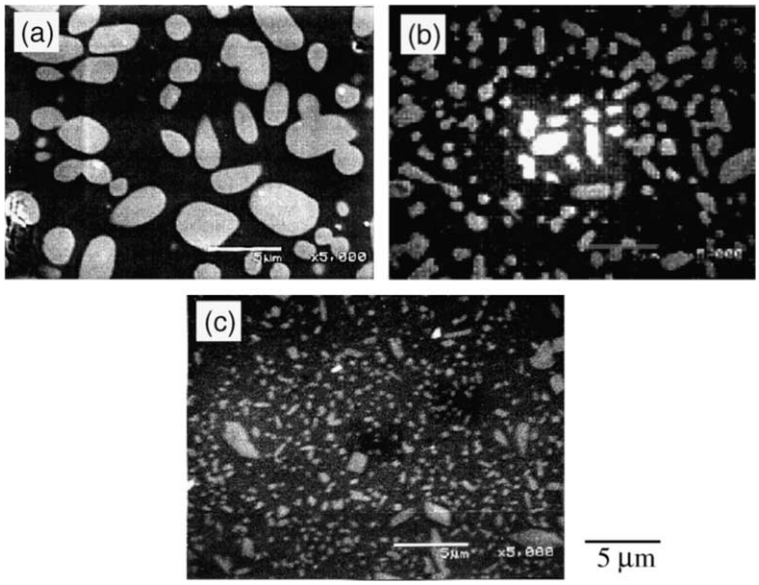

Fig. 1. SEM photographs for the polished surfaces of Gd–Ba–Cu–O bulk samples fabricated using different Gd211 starting powders; (a) Gd211-A; (b) Gd211-B; and (c) Gd211-C listed in Table 1.

which was then melt-processed in 99%Ar–1%O_2 mixture gas. The pellets were partially melted at 1080 °C for 30 min, slowly cooled from 1000 to 960 °C at a rate of 1 °C /h, and finally cooled to room temperature.

Fig. 1 shows SEM (scanning electron microscope) photographs of the polished surface of the melt-textured samples. One can see that the Gd211 particles can be refined by decreasing the particle size of Gd211 starting powders. In particular, the average diameter of Gd211 inclusions in the sample made from the ultra-fine powder of Gd211-C was reduced to sub-micron level as shown in Fig. 1(c).

The observation of Gd211 particles at the partial melting stage will be informative for understanding the difference in the final microstructure. Thus the samples were quenched to room temperature after melted at 1100 °C for 30 min. Fig. 2 shows SEM photographs of the melt-quenched samples prepared from the Gd211 starting powders, Gd211-A and C. The morphology and the size of Gd211 particles at the partial melting stage depended on the size of initially-added Gd211 particles. Rod-like Gd211 particles are observed in the sample made from Gd211-A as shown in Fig. 2(a). In contrast, many fine Gd211 needles were formed in the sample made from Gd211-C powder as shown in Fig. 2(b). From these results, it is proposed that an addition of fine Gd211 powders increased the number of nucleation sites for Gd211 during the peritectic decomposition of Gd123 phase. This will lead to fine dispersion of the resulting Gd211 inclusions in the melt-textured bulk sample as presented in Fig. 1(c).

Superconducting properties were characterized with the specimens of $1.5\times1.5\times1.0$ mm^3 cut from the melt-grown blocks. After the specimens were annealed in oxygen atmosphere at 400 °C for 100 h, the measurements of critical temperature (T_c) and J_c were performed with a SQUID magnetometer. DC-susceptibility measurements showed that onset T_c of all the samples was about 92 K with a sharp transition. Fig. 3 shows the J_c–B

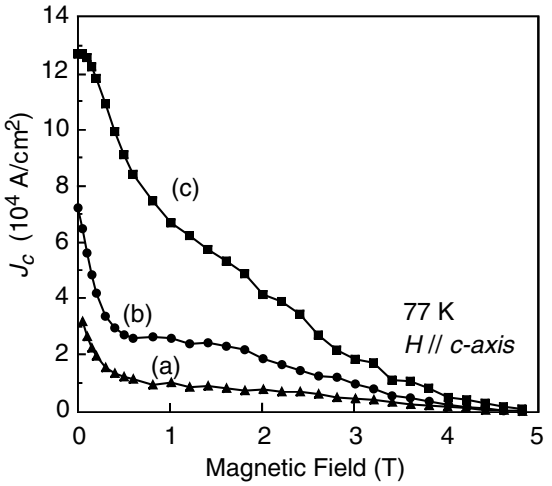

Fig. 3. J_c–B curves at 77 K for the Gd–Ba–Cu–O bulk samples fabricated using (a) Gd211-A, (b) Gd211-B and (c) Gd211-C powders listed in Table 1.

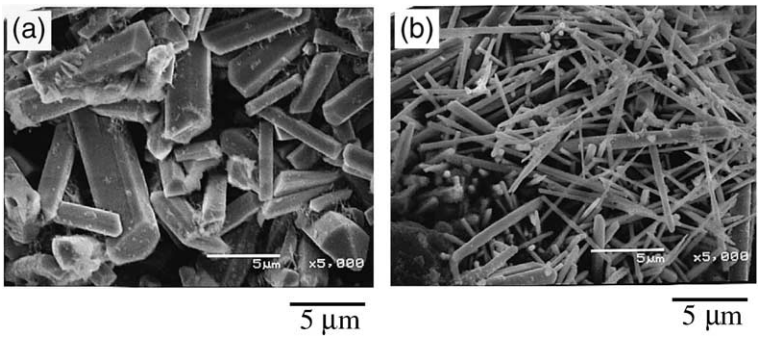

Fig. 2. SEM photographs for the fracture surfaces of melt-quenched samples prepared using (a) Gd211-A and (b) Gd211-C powders listed in Table 1.

curves at 77 K. It is worth nothing that a large increase in J_c was achieved with the size reduction of Gd211. The J_c of the sample with Gd211-C powder exhibited a high value of 1.3×10^5 A/cm^2 at 77 K in self-field. Fig. 4 displays the J_c values at 0.05 T as a function of V_f/d, where V_f is the volume fraction of Gd211 phase and d is their mean size. V_f/d corresponds to the effective interface area of Gd211/Gd123 per unit volume. A linear relation between J_c and V_f/d suggests that the dominant pinning in a low field region is Gd123/Gd211 interfacial pinning [8].

Similar approaches to reduce RE211 particle size were adapted to the other RE–Ba–Cu–O systems [9]. Fig. 5 reveals the relationship between the size of RE211 starting powder and the mean diameter of RE211 inclusions. In the cases of Eu–Ba–Cu–O and Sm–Ba–Cu–O systems, the employment of fine RE211 starting powder was not so effective for the size reduction of RE211 particles in the bulk samples, since the large solubility of these RE elements [10] increases a growth rate of RE211 particles during partial melting. However, in the Y–Ba–Cu–O and Dy–Ba–Cu–O systems, the size of RE211 particles reduced by decreasing the size of RE211 starting powder like Gd–Ba–Cu–O.

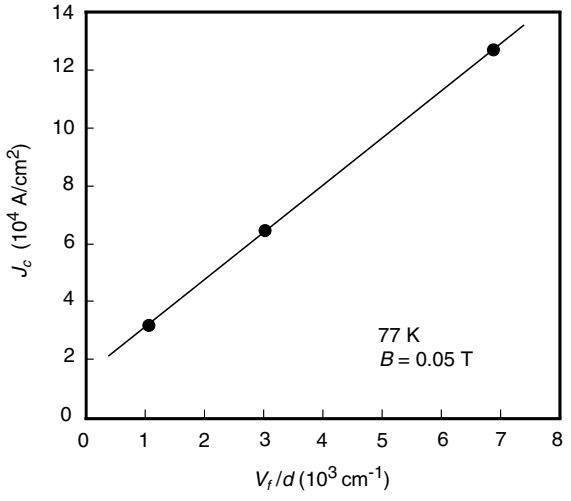

Fig. 4. Plot of the J_c at 0.05 T versus V_f/d of Gd211 particles in Gd–Ba–Cu–O samples.

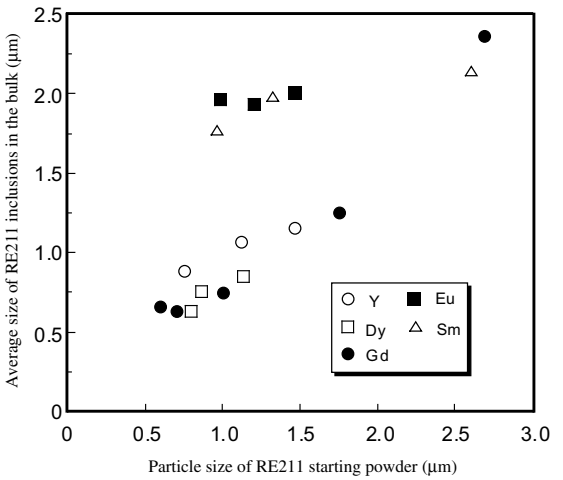

Fig. 5. Relationship between the particle size of the RE211 starting powder and the average size of RE211 inclusions trapped in RE123 matrix phases (RE: Y, Dy, Gd, Eu, Sm).

3. Fabrication and properties of Y–Ba–Cu–O superconductor with fine Y211 particles

On the basis of the experimental results for Gd–Ba–Cu–O, it is evident that the employment of ultra-fine RE211 powders is very effective in further enhancing J_c–B properties. Hence, we attempted the enhancement of J_c for Y–Ba–Cu–O with an employment of finely-milled Y211 powders as starting materials.

For the preparation of Y211 starting powders, the mixed powders of Y_2O_3, BaO_2 and CuO were calcined at 870 °C for 8 h and then milled with ZrO_2–Y_2O_3 balls. As shown in Table 2, the diameter of Y211 powder was reduced down to 0.07 μm with ball-milling. These Y211 powders

Table 2
Y211 starting powders

Y211 powder	Ball-milling time of Y211 starting powder (h)	Particle size of Y211 starting powder (μm)
Y211-A	0	1.36
Y211-B	0.5	0.31
Y211-C	1.0	0.20
Y211-D	2.0	0.11
Y211-E	4.0	0.07

were mixed with Y123 powder and 0.5 wt% Pt in a molar ratio of Y123:Y211 = 100:40. The samples 16 mm in diameter were synthesized with a cold-seeding method in air. Nd123(0 0 1) bulk seed crystal was placed on the top of the pellet. The precursor was heated to 1030 °C and held for 30 min, cooled to 1000 °C in 1h, and then slowly cooled at a rate of 0.3–0.75 °C/h to 960 °C and finally cooled to room temperature. The samples were annealed in flowing oxygen at temperatures at 450 °C for 100 h.

The melt-textured samples were confirmed to be single-grain except for the sample employing Y211-E powder, in which many small grains formed due to undesirable spontaneous nucleation. Fig. 6 shows the SEM photographs of the regions near the seed and the upper side for the sample with Y211-C powder. As shown in Fig. 6(b), the size of Y211 particles were reduced less than 1 μm thanks to the employment of finely-milled Y211 powder. However, the size reduction of Y211 led to inhomogeneous microstructure. When the sample was fabricated by employing the Y211 powders milled for 1 and 2 h (Y211-C and D), few Y211 inclusions were found in the position around the seed as displayed in Fig. 6(a). Such behavior is known as the trapping/pushing phenomena of Y211 [11,12]. The Y211 particles are pushed out from a solidification front, when the Y211 particle is fine and the growth of Y123 crystal is slow (small undercooling).

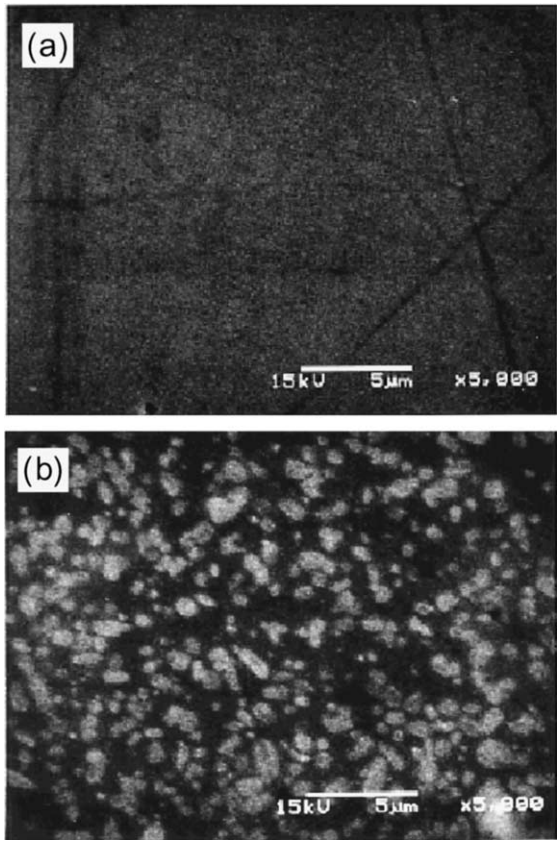

Fig. 6. SEM photographs of Y–Ba–Cu–O samples fabricated by employing Y211-C starting powder listed in Table 2. Photo (a) reveals the regions near the seed crystal, and photo (b) the upper side of the samples.

From SQUID measurements, the onset-T_c was determined to be 90–91 K for all Y–Ba–Cu–O samples. Fig. 7 shows the J_c–B curves at 77 K for the specimens cut from the position near the seed crystal and the upper side area of bulk materials. In Fig. 7(a), it should be noted that the specimens made from Y211-C and D starting powders exhibited the lower J_c values in a low field region accompanied by a large secondary peak effect. Similar large peak effect was reported in Y123 single crystals [13] and the melt-textured Y–Ba–Cu–O, Dy–Ba–Cu–O and Ho-Ba-Cu-O with a low content of RE211 phase [14–16], which is presumably ascribed to a spatial variation in oxygen vacancies. In these samples, a small content of Y211 particles was probably responsible for the large peak effect. As shown in Fig. 7(b), the J_c value of the specimen cut from the upper side area increased with reducing the size of Y211 starting powder. A large increase in J_c was achieved in the sample fabricated with ball-milled Y211 starting powders as well as Gd–Ba–Cu–O. In particular, the sample made from Y211-C powder exhibited a high J_c value of 1.1×10^5 A/cm^2 at 77 K in self-field. In the case of the sample made from Y211-D powder, inhomogeneous distribution of Y211 particles was more remarkable. The volume fraction of Y123 phase in the upper side area largely decreased with the pushing of Y211 particles. This leads to lowering of J_c

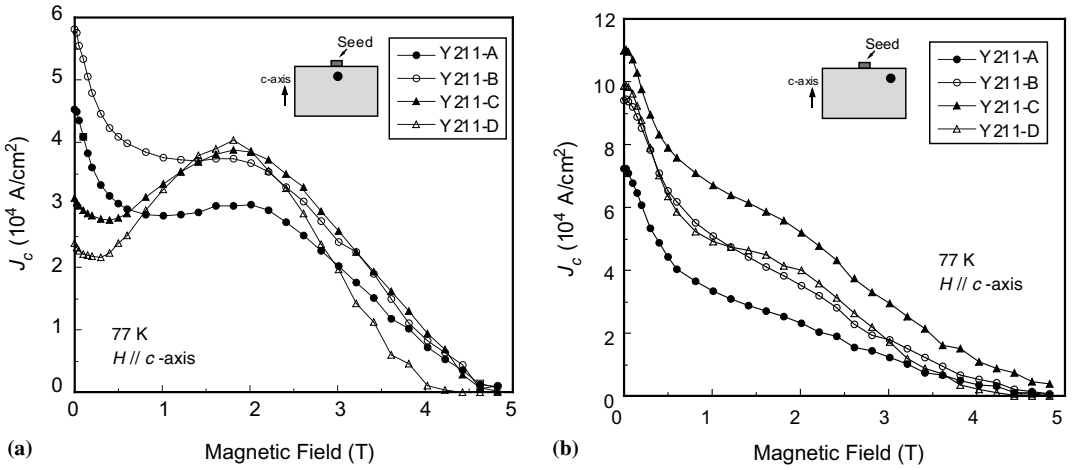

Fig. 7. J_c–B curves at 77 K for the specimens cut from (a) the region near the seed crystal and (b) the upper side area of Y–Ba–Cu–O bulk samples fabricated from various Y211 starting powders.

value compared with that for the sample made from Y211-C.

The enhancement of J_c value leads to improvement in field trapping capability. Hence, we also fabricated large single-grain Y–Ba–Cu–O bulk samples with employing Y211-A and C powders by a hot-seeding method in air. The trapped field of the bulk samples was measured at the gap distance of 1.2 mm from the sample surface [17]. Figs. 8(a) and (b) reveal the contour plots showing trapped field distribution for the samples 33 mm in diameter. The field profile for the sample with Y211-A powder is perfectly symmetric; in contrast the sample fabricated from Y211-C powder exhibited some irregularity in the profile due to the presence of the weak link as indicated by the arrow in Fig. 8(b). In this sample, the low content of Y211 particles around a seed crystal probably caused small crack formation and a decrease in the J_c value in a low field region, which resulted in the drop in the trapped field. To avoid the crack formation, 10 wt% of Ag_2O was added to the samples. Figs. 8(c) and (d) show the trapped field distribution of the Ag-added samples. From the contour plot of the sample with Y211-C powder (Fig. 8(d)), one can see there is still some disorder in the profile; however the weak link nature was evidently improved with Ag addition. This sample could trap a high field of 1.42 T at 1.2 mm above the sample surface.

4. J_c enhancement in (Gd,Y)–Ba–Cu–O and other materials

We also investigated the J_c properties of (Gd,Y)–Ba–Cu–O materials fabricated from Gd123-Y211 precursors. The fine Y211 powders listed in Table 2 were mixed with Gd123 powder and 0.5 wt% Pt in a molar ratio of Gd123:Y211 = 100:40. Melt-processing of the precursor of 20 mm diameter was performed in air by a cold-seeding method using Nd123 seed crystal. All samples were grown as a single-grain, although ultra-fine Y211-E was used as a precursor powder.

Fig. 9 shows SEM photographs of the upper side area of melt-grown (Gd,Y)-Ba-Cu-O. In this system, the employment of fine Y211 starting powder was more effective in reducing 211 inclusions. As shown in Fig. 9(b), the size of 211 particles was reduced down to approximately 300 nm. Fig. 10 shows the J_c–B curves at 77 K for the specimens cut from the (Gd,Y)–Ba–Cu–O samples. The size reduction of 211 particles resulted in

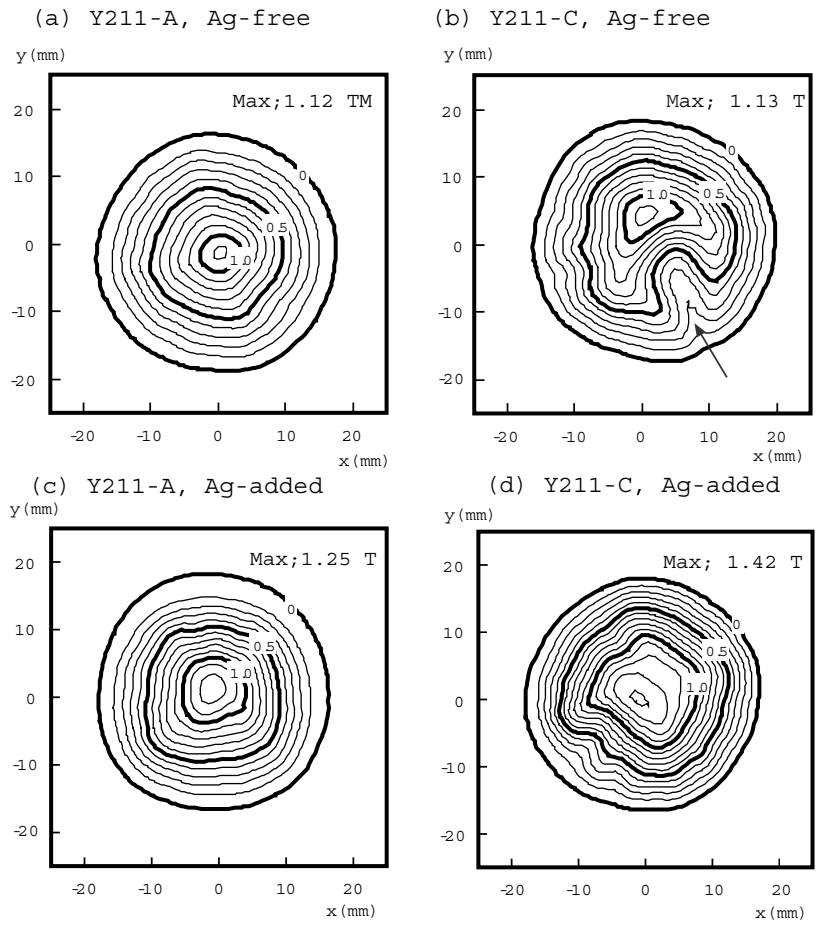

Fig. 8. Contour maps showing trapped field distributions at 77 K for the Ag-free and Ag-added Y–Ba–Cu–O samples fabricated from the starting powders of Y211-A and C. Measurements of trapped field were performed by scanning a Hall probe sensor 1.2 mm above the sample surface.

a drastic enhancement of J_c values. The J_c value of the sample with Y211-E powder reached 2×10^5 A/cm^2 at 77 K in self-field.

Fig. 11 shows the J_c–B curves for (a) (Gd,Y)–Ba–Cu–O, (b) (Gd,Dy)–Ba–Cu–O and (c) (Sm,Y)–Ba–Cu–O. (Gd,Y)–Ba–Cu–O material was synthesized from the precursor with the composition of Gd211:Y211 = 100:20, containing Pt and CeO_2. Melt-processing was performed in 99%Ar–1%O_2 mixture gas. The J_c value reached an extremely high value of 2.5×10^5 A/cm^2 at 77 K, 0.1 T. (Gd,Dy)–Ba–Cu–O and (Sm,Y)–Ba–Cu–O materials were prepared from the precursors with the composition of Gd123:Dy211 = 100:40 and Sm123:Y211 = 100:40. These samples also exhibited high J_c values with the employment of ultra-fine Y211 and Dy211 starting powders. We believe that the J_c value will further be enhanced by the optimization of experimental conditions such as the selection of rare earth elements, the size and amount of RE211 powder and the growth atmosphere.

5. Summary

For the purpose of size reduction of RE211 particles in melt-textured bulk superconductor, we employed the ultra-fine RE211 starting powder as a precursor. We succeeded in enhancing J_c values

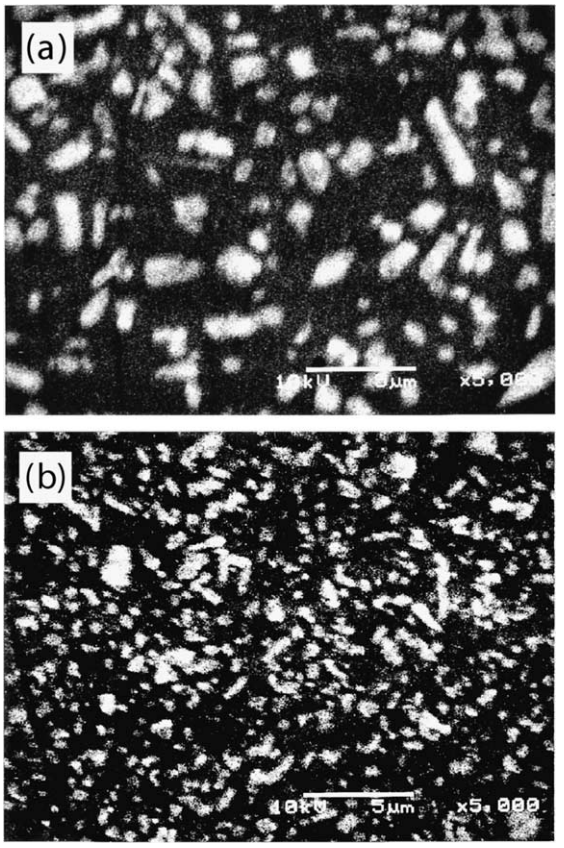

Fig. 9. SEM photographs of (Gd,Y)–Ba–Cu–O materials fabricated from the precursors with the composition of Gd123:Y211 = 100:40, containing (a) Y211-A and (b) Y211-E starting powders.

of melt-textured Gd–Ba–Cu–O and Y–Ba–Cu–O superconductors through the dispersion of fine RE211 inclusions in the matrix. The values of J_c for these materials exceeded 1×10^5 A/cm^2 at 77 K in self-field. In the case of Y–Ba–Cu–O, however, the size reduction of Y211 led to inhomogeneous distribution of Y211 particles, in which the volume fraction of Y211 phase largely decreased near a seed crystal. We also studied the superconducting properties of (Gd,Y)–Ba–Cu–O bulk material fabricated from the precursor of Gd123-Y211. The employment of ultra-fine Y211 powders resulted in a drastic enhancement of J_c values in this system. The maximum J_c for (Gd,Y)–Ba–Cu–O reached 2.5×10^5 A/cm^2 at 77 K and 0.1 T.

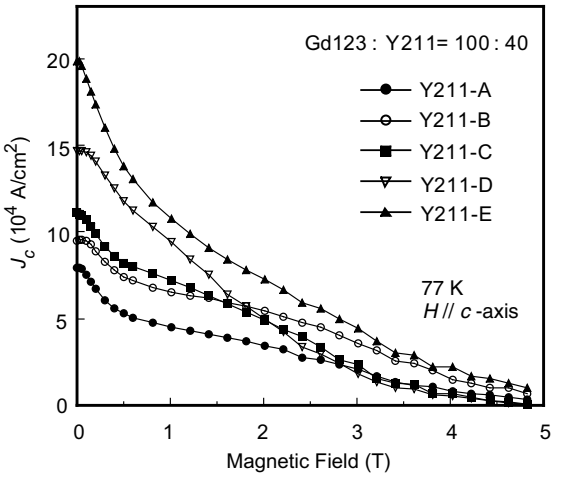

Fig. 10. J_c–B curves at 77 K for the sample fabricated from the precursor Gd123:Y211 = 100:40 in air, in which various Y211 starting powders listed in Table 2 were employed.

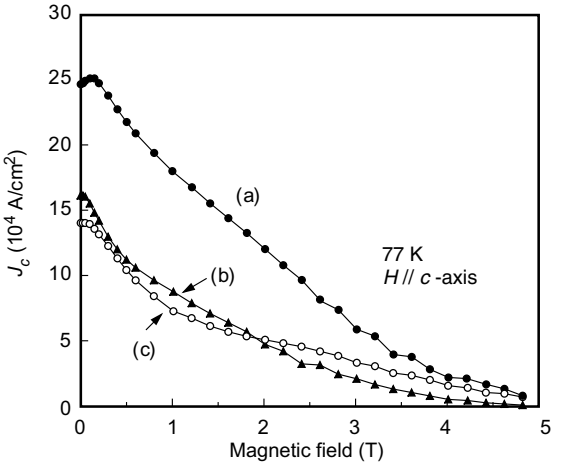

Fig. 11. J_c–B curves at 77 K for the samples fabricated from the precursors with the composition of (a) Gd123:Y211 = 100:20, (b) Gd123:Dy211 = 100:40 and (c) Sm123:Y211 = 100:40.

Acknowledgements

This work is supported by the New Energy and Industrial Technology Development Organization (NEDO).

References

[1] S. Nariki, S.J. Seo, N. Sakai, M. Murakami, Supercond. Sci. Technol. 13 (2000) 778.
[2] S. Nariki, N. Sakai, M. Murakami, Physica C 357–360 (2001) 811.
[3] S. Nariki, N. Sakai, M. Murakami, Physica C 341–348 (2000) 2409.
[4] S. Nariki, N. Sakai, M. Murakami, Physica C 357–360 (2001) 629.
[5] S. Nariki, N. Sakai, M. Murakami, Physica C 378–381 (2002) 631.
[6] S. Nariki, N. Sakai, M. Murakami, Supercond. Sci. Technol. 15 (2002) 648.
[7] S. Nariki, N. Sakai, M. Murakami, Supercond. Sci. Technol., in press.
[8] M. Murakami, K. Yamaguchi, H. Fujimoto, N. Nakamura, T. Taguchi, N. Koshizuka, S. Tanaka, Cryogenics 32 (1992) 930.
[9] S. Nariki, N. Sakai, M. Matsui, M. Murakami, Supercond. Sci. Technol. 15 (2002) 679.
[10] M. Kambara, T. Umeda, Y. Shiohara, Bull. Ceram. Soc. Jpn. 32 (1997) 196.
[11] A. Endo, H.S. Chauhan, Y. Shiohara, Physica C 273 (1996) 107.
[12] A. Endo, H.S. Chauhan, T. Egi, Y. Shiohara, J. Mater. Res. 4 (1996) 802.
[13] H. Küpfer, Th. Wolf, C. Lessing, A.A. Zhukov, X. Lancon, R. Meier-Hilmer, W. Schauer, W. Wühl, Phys. Rev. B 58 (1998) 2886.
[14] S. Nariki, M. Murakami, Supercond. Sci. Technol. 15 (2002) 786.
[15] S. Nariki, N. Sakai, M. Murakami, J. Cryog. Soc. Jpn. 37 (2002) 652.
[16] S. Nariki, N. Sakai, M. Murakami, Physica C 392–396 (2003) 516.
[17] K. Nagashima, T. Higuchi, J. Sok, S.I. Yoo, H. Fujimoto, M. Murakami, Cryogenics 37 (1997) 577.